Proc. 40th IEEE Conf. Decision and Control, 2001, p. 2968–2973

Virtual Leaders, Artificial Potentials and Coordinated Control of Groups[1]

Naomi Ehrich Leonard and Edward Fiorelli
Department of Mechanical & Aerospace Engineering
Princeton University
Princeton, NJ 08544
{naomi,eddie}@princeton.edu

Abstract

We present a framework for coordinated and distributed control of multiple autonomous vehicles using artificial potentials and virtual leaders. Artificial potentials define interaction control forces between neighboring vehicles and are designed to enforce a desired inter-vehicle spacing. A virtual leader is a moving reference point that influences vehicles in its neighborhood by means of additional artificial potentials. Virtual leaders can be used to manipulate group geometry and direct the motion of the group. The approach provides a construction for a Lyapunov function to prove closed-loop stability using the system kinetic energy and the artificial potential energy. Dissipative control terms are included to achieve asymptotic stability. The framework allows for a homogeneous group with no ordering of vehicles; this adds robustness of the group to a single vehicle failure.

1 Introduction

In this paper we describe a distributed control approach to coordination of multiple autonomous vehicles based on artificial potentials and *virtual leaders* (or *virtual beacons*). A central objective is to contribute to a methodology for synthesizing robust and scalable control laws that are relatively simple at the individual level but enable the vehicles at the group level to perform with greater functionality and intelligence. Coordinated vehicle group motion has applications in the sea, on land, in the air, the stratosphere and in space.

Biologists who study animal aggregations such as swarms, flocks, schools and herds have observed the remarkable group-level characteristics that are exhibited as "emergent" properties from individual-level behaviors [8, 9]. These include the ability to make very fast and efficient coordinated maneuvers, the ability to quickly process data and a significantly improved decision making ability (as compared to individuals).

The use of artificial potentials in our approach is inspired by the observations and models of the biologists. Groups in nature make use of a distributed control architecture whereby individuals respond to their sensed environment but are constrained by the behavior of their neighbors. Biologists suggest that the following elements are basic to maintaining a group structure: (1) attraction to distant neighbors up to a maximum distance, (2) repulsion from neighbors too close and (3) alignment or velocity matching with neighbors [8].

In our framework, we encode these local traffic rules by means of (local) artificial potentials that define interaction forces between neighboring vehicles. Each of these potentials is a function of the relative distance between a pair of neighbors. At this stage the vehicles are fully actuated so that control forces for an individual can be derived as minus the gradient of the sum of all potentials affecting that individual. In this way the control forces drive the vehicles to the minimum of the total potential. The local potentials can be designed to correspond to a desired vehicle group geometry with some prescribed inter-vehicle spacing. A Lyapunov function for proving stability and robustness of the group motion can then be constructed as the sum of the vehicle kinetic energies and the artificial potential energies.

In addition to inter-vehicle potential fields, we introduce local potential fields associated with moving reference points that we refer to as *virtual leaders* or *virtual beacons* (these are *not* vehicles).The vehicles respond to these virtual beacons much like they respond to real neighbors. The purpose of the virtual leaders or bea-

[1]Research partially supported by the National Science Foundation under grant CCR-9980058, by the Office of Naval Research under grant N00014-98-1-0649 and by Global Aerospace Corporation under prime contract 07600-58 to the NASA Institute for Advanced Concepts (NIAC)/Universities Space Research Association.

cons is to introduce the mission: to direct, herd and/or manipulate the vehicle group behavior.

We emphasize that there is no leader among the vehicles. In fact, there is no ordering of vehicles required; any vehicle is interchangeable with any other. This feature of the approach adds robustness of the group to the failure of an individual vehicle.

In robotics, artificial potentials have been used extensively to produce feedback control laws, e.g. [5, 11], that avoid obstacles. Potential shaping has also been used successfully for stabilization of mechanical systems (see [2] for a survey). Progress has been made in using artificial potentials in group tasks such as in addressing the problem of autonomous robot assembly [6] and the coordination of spacecraft constellations [7]. In the artificial intelligence and computer animation industries, similar heuristic traffic rules are imposed in order to yield life-like coordinated behaviors [10].

The framework presented herein is applicable to motion in 3D, although we specialize to 2D motion for our case studies. Orientation matching in SE(3) is treated in [12]. In [12] artificial potentials are introduced as a function of relative orientation of pairs of vehicles.

2 Multiple-Vehicle Control System

We consider a group of n vehicles and m virtual leaders (beacons) moving together as shown in Figure 2.1. In this figure the black circles represent vehicles ($n = 8$), and the shaded circles represent virtual leaders ($m = 3$). The control forces applied to a given vehicle are illustrated for the vehicle in the upper left of the figure. These include an interaction force between the vehicle and any neighboring vehicle. The interaction force is a central force that derives from an artificial potential and has magnitude f_I. The corresponding potential V_I and thus the force f_I depend upon the distance r_{ij} between the vehicle i and its neighbor vehicle j (see Figure 2.2). The bottom right plot in Figure 2.1 illustrates the form of f_I that we consider where d_0 and d_1 are scalar constants. As indicated, if $r_{ij} < d_0$ then $f_I < 0$ and the ith and jth vehicles are repelled from each other. If $d_0 < r_{ij} < d_1$ then $f_I > 0$ and the ith and jth vehicles are attracted to each other. If $r_{ij} \geq d_1$ then $f_I = 0$ and the ith and jth vehicles do not affect each other. An example of a potential V_I is

$$V_I = \begin{cases} \alpha_I \left(\ln(r_{ij}) + \frac{d_0}{r_{ij}}\right) & 0 < r_{ij} < d_1 \\ \alpha_I \left(\ln(d_1) + \frac{d_0}{d_1}\right) & r_{ij} \geq d_1 \end{cases}$$

where α_I is a scalar control gain. Throughout we will use the notation $f_I = \nabla_{r_{ij}} V_I$ to imply that at the non-smooth point, $r_{ij} = d_1$, we take $f_I = 0$. In other words $f_I = \nabla_{r_{ij}} V_I$ is as shown in Figure 2.1 and equivalent to the discontinuous function

$$f_I = \begin{cases} \nabla_{r_{ij}} V_I & 0 < r_{ij} < d_1 \\ 0 & r_{ij} \geq d_1 \end{cases}$$

Note that $f_I = 0$ at $r_{ij} = d_0$, i.e., V_I has a global minimum at $r_{ij} = d_0$. Further, f_I in this case gets infinitely large as r_{ij} approaches 0. This helps prevent vehicle collisions. (We note that one can smooth the potential V_I and produce a continuous function f_I).

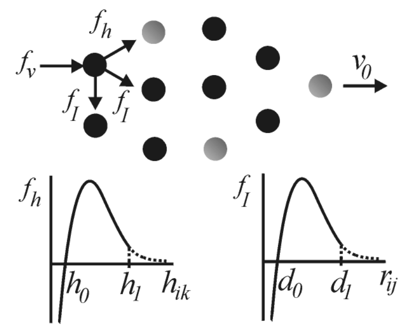

Figure 2.1: Group formation with control forces.

In addition to inter-vehicle forces there is a force of magnitude f_h on a given vehicle associated with any nearby virtual leader. f_h is defined similarly to f_I except that it defines the force on the ith vehicle in reference to the kth virtual leader. For example, we can define the potential V_h from which this force derives as

$$V_h = \begin{cases} \alpha_h \left(\ln(h_{ik}) + \frac{h_0}{h_{ik}}\right) & 0 < h_{ik} < h_1 \\ \alpha_h \left(\ln(h_1) + \frac{h_0}{h_1}\right) & h_{ik} \geq h_1 \end{cases}$$

where α_h is a scalar control gain and h_{ik} is the distance between the ith vehicle and the kth virtual leader (see Figure 2.2). Analogous to the inter-vehicle force, the magnitude $f_h = \nabla_{h_{ik}} V_h$ is given by

$$f_h = \begin{cases} \nabla_{h_{ik}} V_h & 0 < h_{ik} < h_1 \\ 0 & h_{ik} \geq h_1 \end{cases}$$

A controlled dissipative force $\boldsymbol{f_v}$ is also applied to the vehicle. The dissipative force is designed to be zero when the vehicle is moving at a desired velocity $\boldsymbol{v_d}$ (or possibly only at a desired speed v_d). In §4, we will use the Lyapunov stability proof to dictate the form of the dissipative force.

Let $\boldsymbol{b_i} \in \mathbb{R}^3$ be the position of the ith vehicle with respect to an inertial frame for $i = 1, \ldots, n$ as shown in Figure 2.2. The absolute velocity of the ith vehicle is defined as $\boldsymbol{v}_i = \dot{\boldsymbol{b}}_i$. We assume fully actuated vehicles so that the system dynamics take the form:

$$\begin{aligned} \dot{\boldsymbol{b}}_i &= \boldsymbol{v_i} \\ \dot{\boldsymbol{v}}_i &= \boldsymbol{u_i} \end{aligned}$$

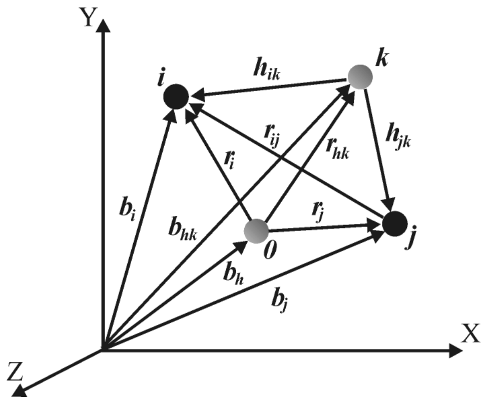

Figure 2.2: Notation for framework.

$i = 1, \ldots, n$. $\boldsymbol{u_i}$ is a control force on the ith vehicle.

Since it will often be of interest to consider the case in which the group of vehicles moves with a virtual leader which is driven at a velocity $\boldsymbol{v_0}(t)$, we affix a coordinate frame with origin at a virtual leader (denoted 0 on Figure 2.2) which has axes aligned with the inertial coordinate frame and does not rotate. The position of the ith vehicle relative to 0 is denoted $\boldsymbol{r_i}$ and the velocity of the ith vehicle relative to 0 is $\dot{\boldsymbol{r}}_{\boldsymbol{i}} = \boldsymbol{v_i} - \boldsymbol{v_0}$. The equations of motion in these coordinates are

$$\frac{d}{dt}\begin{pmatrix} \boldsymbol{r_i} \\ \dot{\boldsymbol{r}}_{\boldsymbol{i}} \end{pmatrix} = \begin{pmatrix} \dot{\boldsymbol{r}}_{\boldsymbol{i}} \\ \boldsymbol{u_i} - \dot{\boldsymbol{v}}_{\boldsymbol{0}} \end{pmatrix} \tag{2.1}$$

for $i = 1, \ldots, n$. Note that the vector $\boldsymbol{r_{ij}} = \boldsymbol{r_i} - \boldsymbol{r_j}$ so that the control force $\boldsymbol{u_i}$ is given as

$$\begin{aligned} \boldsymbol{u_i} &= -\sum_{j\neq i}^{n} \nabla_{\boldsymbol{r_i}} V_I(r_{ij}) - \sum_{k=0}^{m-1} \nabla_{\boldsymbol{r_i}} V_h(h_{ik}) + \boldsymbol{f_{v_i}} \quad (2.2) \\ &= -\sum_{j\neq i}^{n} \frac{f_I(r_{ij})}{r_{ij}} \boldsymbol{r_{ij}} - \sum_{k=0}^{m-1} \frac{f_h(h_{ik})}{h_{ik}} \boldsymbol{h_{ik}} + \boldsymbol{f_{v_i}} \end{aligned}$$

where we identify $\boldsymbol{h_{i0}} \equiv \boldsymbol{r_i}$. This control law can easily be modified to allow for different potentials associated with different virtual leaders if desired.

3 Steady Motions: Schooling and Flocking

In this section we illustrate the framework and its features by presenting several examples of flocking and schooling. We refer to a *schooling* maneuver as a steady group translation, e.g., where the center of mass of the group translates. A *flocking* maneuver refers to a motion in which the vehicles circle a stationary point such that the center of mass of the group is stationary. To illustrate these maneuvers, we consider the case in which the velocity of the moving frame (i e., the 0th virtual leader) $\boldsymbol{v_0}$ is constant. We also specialize to 2D space.

Consider polar coordinates defined as follows:

$$\boldsymbol{r_i} = \begin{pmatrix} r_i \cos\theta_i \\ r_i \sin\theta_i \end{pmatrix}, \quad \boldsymbol{r_{hk}} = \begin{pmatrix} r_{hk} \cos\theta_{hk} \\ r_{hk} \sin\theta_{hk} \end{pmatrix}.$$

Further, we have the relations

$$\begin{aligned} r_{ij}^2 &= r_i^2 + r_j^2 - 2r_i r_j \cos(\theta_i - \theta_j) \\ h_{ik}^2 &= r_i^2 + r_{hk}^2 - 2r_i r_{hk} \cos(\theta_i - \theta_{hk}). \end{aligned}$$

In the case in which

$$\boldsymbol{f_{v_i}} = \frac{f_v(v_i)}{v_i} \boldsymbol{v_i}, \tag{3.1}$$

the equations of motion (for $r_i \neq 0$) become

$$\begin{aligned} \ddot{r}_i &= r_i\dot{\theta}_i^2 - \sum_{j\neq i}^{n} (r_i - r_j \cos(\theta_i - \theta_j)) \frac{f_I(r_{ij})}{r_{ij}} - f_h(r_i) \\ &\quad - \sum_{k=1}^{m-1} (r_i - r_{hk} \cos(\theta_i - \theta_{hk})) \frac{f_h(h_{ik})}{h_{ik}} \\ &\quad + (\dot{r}_i + v_{0_x} \cos\theta_i + v_{0_y} \sin\theta_i) \frac{f_v(\dot{\boldsymbol{r}}_{\boldsymbol{i}} + \boldsymbol{v_0})}{\|\dot{\boldsymbol{r}}_{\boldsymbol{i}} + \boldsymbol{v_0}\|} \quad (3.2) \\ r_i\ddot{\theta}_i &= -2\dot{r}_i\dot{\theta}_i - \sum_{j\neq i}^{n} r_j \sin(\theta_i - \theta_j) \frac{f_I(r_{ij})}{r_{ij}} \\ &\quad - \sum_{k=1}^{m-1} r_{hk} \sin(\theta_i - \theta_{hk}) \frac{f_h(h_{ik})}{h_{ik}} \\ &\quad + (r_i\dot{\theta}_i + v_{0_y} \cos\theta_i - v_{0_x} \sin\theta_i) \frac{f_v(\dot{\boldsymbol{r}}_{\boldsymbol{i}} + \boldsymbol{v_0})}{\|\dot{\boldsymbol{r}}_{\boldsymbol{i}} + \boldsymbol{v_0}\|} \quad (3.3) \end{aligned}$$

for $i = 1, \ldots, n$.

3.1 Flocking

Our model of flocking is similar in spirit to that described in [3]. We consider a dissipation model of the form (3.1) where $f_v(v_i) = -a(v_i - v_d)$ where $a > 0$. We take $\boldsymbol{v_0} = 0$ and $v_d \neq 0$.

Case F1: $\boldsymbol{n = m = 1}$. Consider the case of one vehicle and one stationary virtual leader. For steady circular flight around the virtual leader at 0 ($\dot{\theta}$ and r are constant), we take $\dot{r} = \ddot{r} = \ddot{\theta} = 0$. Substituting into the equations of motion we get $r\dot{\theta}^2 - f_h(r) = 0$ and $f_v(v) = 0$. So, at the steady motion, $v = v_d$. In particular, $v_d^2 = v^2 = r^2\dot{\theta}^2$ and thus $f_h(r) = v_d^2/r$. For f_h of the form shown in Figure 2.1 and for small enough v_d there will be two solutions $r = r_{e_1}, r_{e_2}$ where $r_{e_1} < r_{e_2}$. It has been shown by linearization at these two solutions that the solution corresponding to $r = r_{e_1}$ and $\dot{\theta} = v_d/r_{e_1}$ is stable while the solution at $r = r_{e_2}$ is unstable [4].

Case F2: $\boldsymbol{n = N, m = 1}$. For N vehicles circling a single stationary virtual leader, symmetrical uniformly rotating rings can be constructed by selecting d_0 such that the vehicles are arranged at the vertices of an N-sided inscribed polygon. In this case, azimuthal forces are automatically balanced by symmetry and d_1 is selected small enough such that only nearest neighbor interaction is allowed.

3.2 Schooling

In the case of schooling, we assume that the desired vehicle velocity $\boldsymbol{v_d} = \boldsymbol{v_0}$, the velocity of the 0th virtual leader. Other virtual leaders will also be moved with velocity $\boldsymbol{v_0}$ so that in steady motions, vehicles and virtual leaders will move as a group as illustrated in Figure 2.1.

Case S1: $\boldsymbol{n = m = 1}$. In this case we have a schooling solution when $\dot{\theta} = \ddot{\theta} = \dot{r} = \ddot{r} = 0$. Substituting into (3.2) and (3.3) gives $\boldsymbol{f_v}(\boldsymbol{v}) = 0$ and $f_h(r) = 0$. Because θ is arbitrary there is an S^1 symmetry. The solution of interest is $r = h_0$ and $\boldsymbol{v} = \boldsymbol{v_0}$. This corresponds to the vehicle positioned somewhere on the circle about 0 of radius h_0 moving with the same velocity as the virtual leader. There will also be steady solutions for $r > h_1$ since $f_h = 0$ there. However, an additional virtual leader could be added to avoid such solutions.

Case S2: $\boldsymbol{n = 2}$, $\boldsymbol{m = 1}$. In this case we have two vehicles which can interact and a single virtual leader which can influence both vehicles (we take d_1 and h_1 to be relatively large). Consider equilibria that correspond to $\dot{r}_i = \dot{\theta}_i = \ddot{r}_i = \ddot{\theta}_i = 0$ and $\boldsymbol{v_i} = \boldsymbol{v_d} = \boldsymbol{v_0}$ for $i = 1, 2$. Then, from (3.2) and (3.3) with any model of dissipation that is zero when $\boldsymbol{v_i} = \boldsymbol{v_d}$ and with $d_0 \leq 2h_0$, an equilibrium solution is given by $r_1 = r_2 = h_0$ and $r_{12} = d_0$. This corresponds to both vehicles positioned on the circle about 0 of radius h_0 and a distance d_0 apart from each other. The two vehicles and the virtual leader move together in this arrangement with velocity $\boldsymbol{v_0}$. As in the one-body case, there is again an S^1 symmetry: there is a family of solutions parameterized by the angle θ_1 (or θ_2). Two such solutions are illustrated in Figure 3.1(a) and (b). The only other nearby equilibria correspond to $\theta_1 = \theta_2$

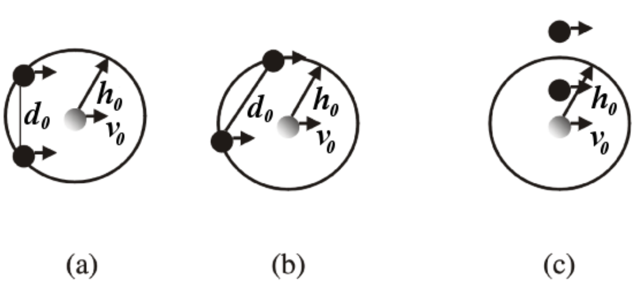

Figure 3.1: Equilibrium solutions for two bodies and one virtual leader.

and $f_h(r_1) = -f_h(r_2) = f_I(r_{12})$ where without loss of generality we have taken $r_2 > r_1$. Again there is an S^1 family of these equilibria. One such equilibrium is shown in Figure 3.1(c). This type of equilibrium solution is unstable whereas the solutions of the form shown in Figure 3.1(a) and (b) are stable (see §4).

Case S3: $\boldsymbol{n = m = 2}$. Since the motions in Figure 3.1(a) and (b) represent two qualitatively different maneuvers, it is of interest to introduce a second virtual leader to break the S^1 symmetry. For example, suppose we introduce a second virtual leader a distance $r_{h1} = \sqrt{4h_0^2 - d_0^2}$ from the original virtual leader 0. Then, an equilibrium solution is given by $r_1 = r_2 = h_{11} = h_{21} = h_0$ and $r_{12} = d_0$. This corresponds to the two vehicles positioned at the two points of intersection of circles of radius h_0 about the virtual leaders as shown in Figure 3.2. In Figure 3.2(a),

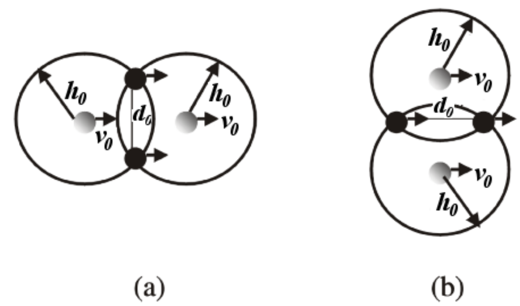

Figure 3.2: Virtual leader for symmetry breaking.

the second virtual leader is placed directly behind the original leader, and in equilibrium the vehicles travel broadside. In Figure 3.2(b), the second virtual leader is placed directly beside the original leader, and in equilibrium the two vehicles travel single file. It is of interest in future work to investigate how to make global formation changes such as switching stably from the maneuver in Figure 3.2(a) to the maneuver in Figure 3.2(b). This case study suggests the possibility of making such a formation change by moving the second virtual leader from its position relative to 0 in Figure 3.2(a) to its relative position in Figure 3.2(b).

Case S4: Equilateral triangle, $\boldsymbol{n = 3}$, $\boldsymbol{m = 1}$. In the case of three vehicles and one virtual leader it is of interest to stabilize the three vehicles moving together in an equilateral triangle formation. We can choose d_1 and h_1 relatively large so that each vehicle sees the virtual leader as well as the other two vehicles. If we let $d_0 = h_0\sqrt{3}$ then there is an equilibrium $r_1 = r_2 = r_3 = h_0$ and $r_{12} = r_{13} = r_{23} = d_0$ (see Figure 3.3). At this equilibrium, the three vehicles lie on the circle of radius h_0 about the virtual leader 0 and a distance d_0 apart from one another. With one virtual leader, there remains an S^1 symmetry (e.g., parametrized by θ_i, $i = 1, 2$ or 3).

Case S5: Hexagonal lattice, $\boldsymbol{n \geq 3}$, $\boldsymbol{m = 1}$. For many vehicles Case S4 can be extended to create an equilibrium formation consisting of vehicles moving together and positioned at the vertices in a hexagonal lattice. As in Case S4 we let $d_0 = h_0\sqrt{3}$. This time, however, we choose $h_1 < d_0\sqrt{3} - h_0$ and $d_1 < d_0\sqrt{3}$. This yields hexagonal lattice equilibria in which $r_{ij} = d_0$ for $i, j = 1, \ldots, n$ as shown in Figure 3.3.

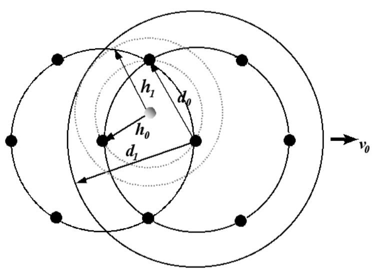

Figure 3.3: Hexagonal lattice of vehicles moving together.

That is, about each vehicle there is a maximum of six vehicles lying evenly space around a circle of radius d_0. Three vehicles can lie in an equilateral triangle on the circle of radius h_0 about the virtual leader 0. Note that near this equilibrium only these three vehicles will be aware of and influenced by the virtual leader. Similarly, near this equilibrium, each vehicle will in general interact with at most six neighboring vehicles.

With one virtual leader there remains an S^1 symmetry. This can be broken with the addition of other virtual leaders. Virtual leaders can furthermore be added to strengthen the attraction to the "core" of the lattice.

Case S6: Group geometry built out of lattice, $n \geq 3$, $m \geq 1$. In the case of many vehicles we can design potentials to stabilize an equilibrium that corresponds to a group geometry of interest such as vehicles moving in a circle (e.g., to escort another vehicle), in a line, in a V-shape, etc. One way to do this is to start with the set-up of Case S5 and add virtual leaders in positions where no vehicle should be present. For example, if we have six vehicles and want them to form a circle, we would place a virtual leader in one of the vehicle positions in the lattice of Figure 3.3. For this virtual leader, assign $h_0 = d_0$ and $h_1 = d_1$. Then, the six vehicles in a circle about this virtual leader are in equilibrium and the virtual leader "uses up" the center space. To keep the circle strongly intact, additional virtual leaders could be added to the ring outside of the circle of six vehicles forcing the vehicles away from that ring and trapping them in their circle.

4 Stability of Schooling Motions

Without dissipation, the schooling equilibria of Cases S1 through S6 (except for the unstable example of Case S2 shown in Figure 3.1(c)) are all locally stable in the sense of Lyapunov. When there is an S^1 symmetry, the stability is modulo S^1. Stability follows because in each of these cases, by design, the equilibrium described is a global minimum of the total artificial potential.

To illustrate we consider Case S2 with two vehicles and one virtual leader and study the equilibrium corresponding to $r_1 = r_2 = h_0$ and $r_{12} = d_0$ shown in Figure 3.1(a) and (b). The dynamics of the controlled system (without dissipation) and near the equilibrium (i.e., away from the discontinuity in f_h and f_I) are described by the Lagrangian

$$
\begin{aligned}
L(r_1, r_2, \theta_1, \theta_2) &= \frac{1}{2}\sum_{i=1}^{2} \dot{\boldsymbol{r}}_i \cdot \dot{\boldsymbol{r}}_i - V(r_1, r_2) \\
&= \frac{1}{2}(\dot{r}_1^2 + r_1^2\dot{\theta}_1^2 + \dot{r}_2^2 + r_2^2\dot{\theta}_2^2) - V(r_1, r_2)
\end{aligned}
$$

where $V(r_1, r_2) = V_I(r_{12}) + V_h(r_1) + V_h(r_2)$.

Define $\theta_{12} = \theta_1 - \theta_2$ and recall that $r_{12}^2 = r_1^2 + r_2^2 - 2r_1r_2\cos\theta_{12}$. In the coordinates $r_1, r_2, \theta_1, \theta_{12}$ we then write the Lagrangian as

$$
\begin{aligned}
L(r_1, r_2, \theta_1, \theta_{12}) &= \frac{1}{2}(\dot{r}_1^2 + r_1^2\dot{\theta}_1^2 + \dot{r}_2^2 + r_2^2(\dot{\theta}_1 - \dot{\theta}_{12})^2) \\
&\quad - V_I(r_{12}(r_1, r_2, \theta_{12})) - V_h(r_1) - V_h(r_2).
\end{aligned}
$$

Since θ_1 is a cyclic variable (our S^1 symmetry), its conjugate momentum $p_{\theta_1} = r_1^2\dot{\theta}_1 = \mu$ is constant. So, the total energy of the reduced system becomes

$$
\begin{aligned}
E(r_1, r_2, \theta_{12}, p_{r_1}, p_{r_2}, p_{\theta_{12}}) &= \frac{1}{2}\left(p_{r_1}^2 + p_{r_2}^2 + \frac{p_{\theta_{12}}^2}{r_2^2}\right) \\
&\quad + V_I(r_{12}(r_1, r_2, \theta_{12})) + V_h(r_1) + V_h(r_2) + \frac{\mu^2}{2r_1^2}.
\end{aligned}
$$

Using E as our Lyapunov function, the equilibrium, $r_1 = r_2 = h_0$, $r_{12} = d_0$, $p_{r_1} = p_{r_2} = p_{\theta_{12}} = 0$ at $\mu = 0$ is a minimum. Thus, we conclude stability of the reduced system which implies stability modulo S^1. When an additional virtual leader is added to break symmetry, stability follows analogously in the full state space.

In the example above, for an equilibrium such that $\mu \neq 0$, the vehicles will be circling the virtual leader while moving with it, i.e., a combined schooling/flocking maneuver. We note that dissipation that depends on absolute velocity will likely destroy such equilibria.

In general, the Lyapunov function corresponding to total kinetic energy plus artificial potential energy (E in the example above) can be used further to select a controlled dissipation force $\boldsymbol{f_v}$ and to prove local asymptotic stability. Consider the general form of this Lyapunov function defined on the full state space as

$$\Phi = \frac{1}{2}\sum_{i=1}^{n}\left(\dot{\boldsymbol{r}}_{\boldsymbol{i}}\cdot\dot{\boldsymbol{r}}_{\boldsymbol{i}} + \sum_{j\neq i}^{n} V_I(r_{ij}) + 2\sum_{k=0}^{m-1} V_h(h_{ik})\right)$$

The derivative of Φ with respect to time is

$$\begin{aligned}\dot{\Phi} &= \sum_{i=1}^{n}\dot{\boldsymbol{r}}_{\boldsymbol{i}}\cdot\left(\boldsymbol{u}_{\boldsymbol{i}} + \sum_{j\neq i}^{n}\nabla_{\boldsymbol{r}_{\boldsymbol{i}}} V_I(r_{ij}) + \sum_{k=0}^{m-1}\nabla_{\boldsymbol{r}_{\boldsymbol{i}}} V_h(h_{ik})\right)\\ &= \sum_{i=1}^{n}\dot{\boldsymbol{r}}_{\boldsymbol{i}}\cdot\boldsymbol{f}_{\boldsymbol{v}_{\boldsymbol{i}}}\end{aligned}$$

where we have used the expression (2.2) for the control law $\boldsymbol{u}_{\boldsymbol{i}}$ and we have assumed there is a neighborhood about the equilibrium in which the control law remains smooth. Thus, if we choose

$$\boldsymbol{f}_{\boldsymbol{v}_{\boldsymbol{i}}} = -a_i\dot{\boldsymbol{r}}_{\boldsymbol{i}}, \quad a_i > 0 \tag{4.1}$$

for $i = 1, \ldots, n$, then $\dot{\Phi}$ is negative definite and equal to zero if and only if $\dot{\boldsymbol{r}}_{\boldsymbol{i}} = 0$ for all i. By the LaSalle Invariance Principle we can conclude that an equilibrium that has been made stable without dissipation will be asymptotically stabilized with this form of dissipation.

Proposition 4.1 *Consider a group of n vehicles with dynamics defined by (2.1), $\boldsymbol{v_0}$ a constant, and the control law given by (2.2) and (4.1). Let the equilibrium of interest be of the form $\dot{\boldsymbol{r}}_{\boldsymbol{i}} = 0$ and $r_i = h_0$ or $r_i > h_1$, $r_{ij} = d_0$ or $r_{ij} > d_1$, and $h_{ik} = h_0$ or $h_{ik} > h_1$ for all $i, j = 1, \ldots, n$, $j \neq i$, and $k = 1, \ldots, m-1$. We assume that h_1 and d_1 have been defined so that there is a neighborhood about the equilibrium in which the control law remains smooth. Then, the equilibrium is a global minimum of the sum of all the artificial potentials and is locally asymptotically stable for the closed-loop dynamics. In the case in which there is no symmetry, stability is achieved in the full state space. In the case in which there is symmetry, the relative velocity of all vehicles will go to zero and each symmetry variable will be stabilized to an arbitrary (constant) value.*

Proposition 4.1 can be used, in particular, to prove asymptotic stability of all of the schooling equilibria described in Cases S1 through S6. This excludes, of course, the unstable example described in Case S2 which can be proved unstable by linearization. More generally it applies to any formation designed according to the very straightforward hypotheses.

5 Final Remarks

In this paper we have presented a framework for coordinated control of a group of vehicles modeled as point masses with full actuation. The approach makes use of artificial potentials and virtual leaders (beacons) to stabilize schooling or flocking motions with prescribed group geometry and inter-vehicle spacing. We have proven local asymptotic stability in the case that a dissipation term is added to the control law.

Simulations of the cases described here verify the stability results and give insight into the influence of control parameters on performance. Performance issues will be further investigated. It is of interest in future work to address global dynamics of the group including an examination of the role of undesirable formations that are also local minima for the designed potentials, and an investigation of switching between different formations. Virtual leaders may prove useful to make switches (see case S3) and also to avoid obstacles, to split and merge subgroups, etc. In current work, we are using the framework to perform gradient climbing, i.e., to efficiently find the densest source of a spatially distributed signal [1].

Other future directions include development of cases in 3D, inclusion of more detailed vehicle dynamics, consideration of underactuated systems and nonholonomic constraints, as well as the coupling of this work with the orientation control approach of [12]. Control laws developed as part of this work will be implemented on the experimental multiple underwater vehicle test-bed currently under development at Princeton.

References

[1] R. Bachmayer and N. E. Leonard. Experimental test-bed for multi-vehicle control, navigation, and communications. In *Proceedings of the UUST*, 2001.

[2] A. M. Bloch, N. E. Leonard, and J. E. Marsden. Controlled Lagrangians and the stabilization of mechanical systems II: Potenital shaping. In *IEEE Transactions on Automatic Control*, 2001. In press.

[3] F. Heppner and U. Grenander. A stochastic nonlinear model for coordinated bird flocks. In *The Ubiquity of Chaos*, pages 233–238. AAAS Publications, 1990.

[4] P.J. Holmes, 2000. Personal Correspondence.

[5] O. Khatib. Real time obstacle avoidance for manipulators and mobile robots. *Int. J. Robotics Research*, pages 90–99, 1986.

[6] D. E. Koditschek. An approach to autonomous robot assembly. *Robotica*, pages 137–155, 1994.

[7] C. R. McInnes. Potential function methods for autonomous spacecraft guidance and control. *Advances in the Astronautical Sciences*, pages 2093–2109, 1996.

[8] A. Okubo. Dynamical aspects of animal grouping: swarms, schools, flocks and herds. *Advances in Biophysics*, pages 1–94, 1985.

[9] J. K. Parrish and W. H. Hammer, editors. *Animal Groups in Three Dimensions*, page 378. Cambridge University Press, 1997.

[10] C. W. Reynolds. Flocks, herds, & schools: a distributed behavioral model. *Computer Graphics*, 21(4):25–34, 1987.

[11] E. Rimon and D. E. Koditschek. Exact robot navigation using artificial potential functions. *IEEE Transactions on Robotics and Automation*, pages 501–518, 1992.

[12] T. R. Smith, H. Hanßmann, and N. E. Leonard. Orientation control of multiple underwater vehicles with symmetry-breaking potentials. In *Proceedings of IEEE CDC*, 2001.